Riemannian Nonlinear Mixed Effects Models: Analyzing Longitudinal Deformations in Neuroimaging

THE UNIVERSITY of WISCONSIN MADISON
WAISMAN CENTER
UF UNIVERSITY of FLORIDA
Hyunwoo J. Kim, Nagesh Adluru, Heemanshu Suri, Baba C. Vemuri, Sterling C. Johnson, Vikas Singh
http://pages.cs.wisc.edu/~hwkim/projects/riem-mem/

The Motivating Problem

- Develop **nonlinear mixed effects models** for responses (Y) that lie on curved spaces such as the manifold of **symmetric positive definite (SPD) matrices**.
- Characterize complex **morphological longitudinal brain changes** using **Cauchy deformation tensors (CDTs)** derived from MRI data.
- Capture **subject-specific** progression rate and disease onset time using non-linear mixed effects models on CDTs

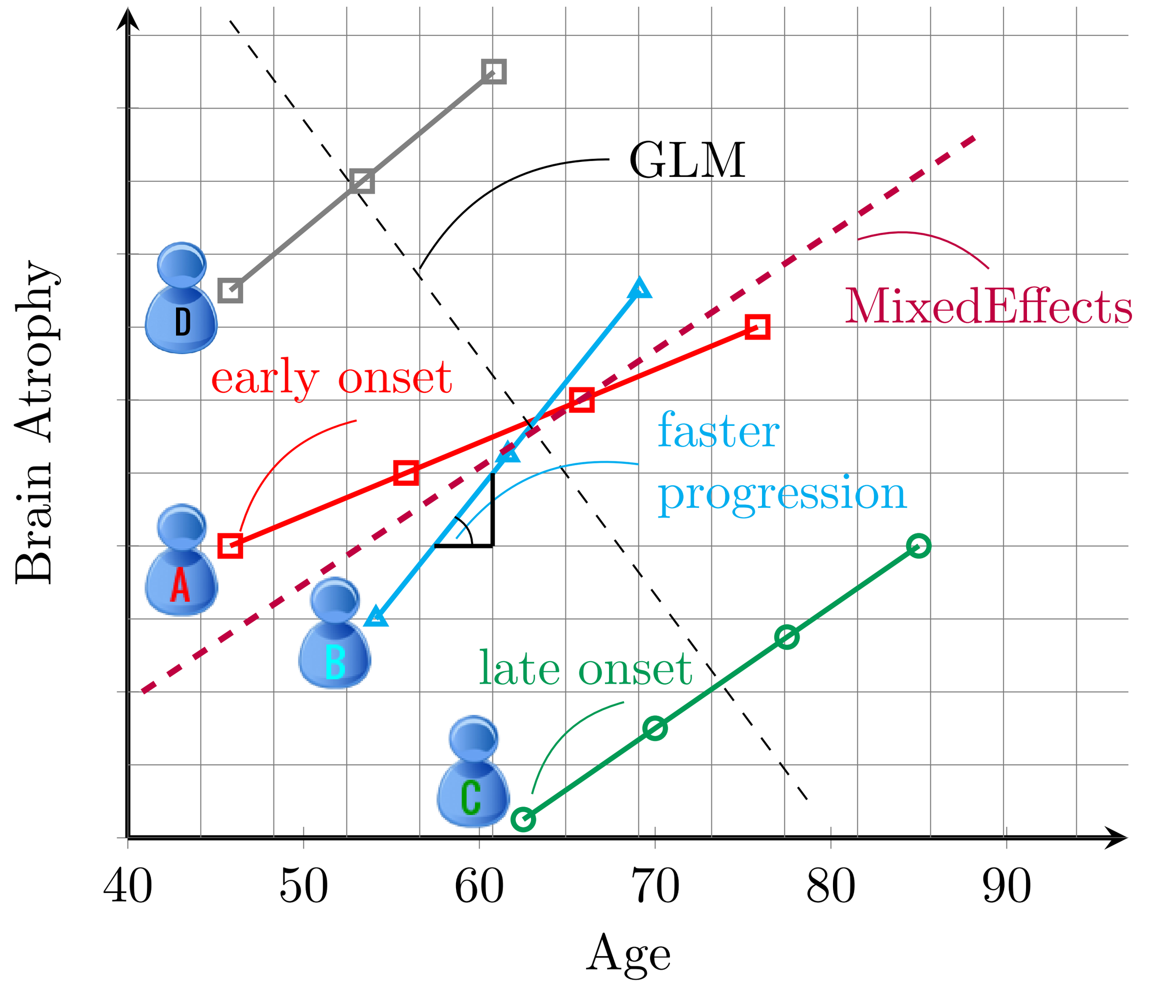

Figure: **Benefits of mixed effects models comparing to fixed effects models (GLM).** Each subject has a different progression rate of brain atrophy (acceleration) and has a different onset for atrophy.

Euclidean Mixed Effects Models

Euclidean linear mixed effects model

$$y_{[\![ij]\!]} = \beta^0 + \beta^1 x^1_{[\![ij]\!]} + \cdots + \beta^p x^p_{[\![ij]\!]} + u^1_i z^1_{[\![ij]\!]} + \cdots + u^q_i z^q_{[\![ij]\!]} + \epsilon_{[\![ij]\!]},$$

$$\text{(OR) } \boldsymbol{y}_i = X_i \boldsymbol{\beta} + Z_i \boldsymbol{u}_i + \epsilon,$$

where $\boldsymbol{x}_{[\![ij]\!]} \in \mathbf{R}^p$, $\boldsymbol{y}_{[\![ij]\!]} \in \mathbf{R}^m$ and $\mathbf{z}_{[\![ij]\!]} \in \mathbf{R}^q$

$\boldsymbol{u}_i$ and ϵ are normally distributed.

Euclidean nonlinear mixed effects model

$$y_{[\![ij]\!]} = \beta_0 + \boldsymbol{\beta}\psi_i(\boldsymbol{x}_{[\![ij]\!]}) + u_i \mathbf{z}_{[\![ij]\!]}, \text{ where } \psi_i(\boldsymbol{x}) := \alpha_i(\boldsymbol{x} - \tau_i - t_0) + t_0.$$

$(\alpha_i, \tau_i, \boldsymbol{u}_i)$ are subject-specific random effects related to acceleration, onset time (time shift), and intercept (spatial shift).

Regression on Manifolds: Basic Operations

Operation	Subtraction	Addition	Distance	Mean	Covariance
Euclidean	$\overrightarrow{x_i x_j} = x_j - x_i$	$x_i + \overrightarrow{x_j x_k}$	$\Vert\overrightarrow{x_i x_j}\Vert$	$\sum_{i=1}^n \overrightarrow{\bar{x} x_i} = 0$	$\mathbb{E}\left[(x_i - \bar{x})(x_i - \bar{x})^T\right]$
Riemannian	$\overrightarrow{x_i x_j} = \mathrm{Log}(x_i, x_j)$	$\mathrm{Exp}(x_i, \overrightarrow{x_j x_k})$	$\Vert\mathrm{Log}(x_i, x_j)\Vert_{x_i}$	$\sum_{i=1}^n \mathrm{Log}(\bar{x}, x_i) = 0$	$\mathbb{E}\left[\mathrm{Log}(\bar{x}, x_i)\mathrm{Log}(\bar{x}, x_i)^T\right]$

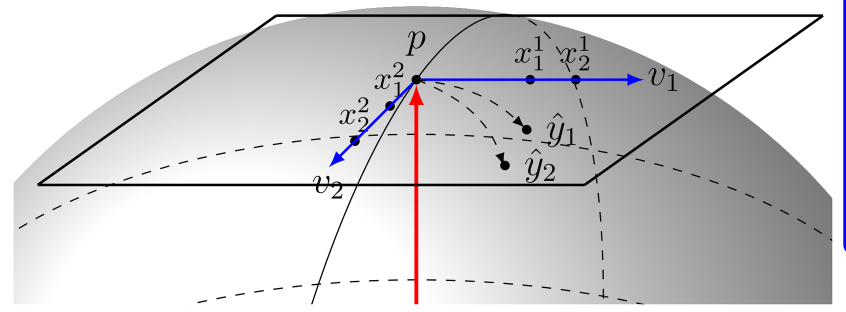

v^1, v^2 are tangent vectors. Each entry of independent variables $(x^1, x^2) \in \mathbf{R}^2$, is multiplied by v_1 and v_2 respectively in $T_p\mathcal{M}$. Here, x^j_i denotes j-th entry of the i-th instance.

Riemannian Mixed Effects Models

Manifold-valued MGLM [1]

$$y = \mathrm{Exp}\left(\mathrm{Exp}\left(p, v^1x^1 + v^2x^2 + \ldots + v^nx^n\right), \epsilon\right),$$

where $\epsilon \sim \frac{1}{Z(\mu,\sigma)} \exp\left(-\frac{d(y,\mu)^2}{2\sigma^2}\right)$ and $Z(\mu,\sigma) = \int_{\mathcal{M}} \exp\left(-\frac{d(y,\mu)^2}{2\sigma^2}\right)$ is the normalization factor.

Riemannian linear mixed effects model

$$y_{[\![ij]\!]} = \mathrm{Exp}(\mathrm{Exp}(B_i(r), \Gamma_{B\to B_i(r)}(V)(\boldsymbol{x}_{[\![ij]\!]} - \tau_i(r))), \epsilon).$$

Riemannian nonlinear mixed effects model (RNLMM)

$$y_{[\![ij]\!]} = \mathrm{Exp}(\mathrm{Exp}(B_i, \Gamma_{B\to B_i}(V)\alpha_i(x_{[\![ij]\!]} - \tau_i - t_0), \epsilon_{ij})))$$

where $B_i = \mathrm{Exp}(B, U_i)$, $\epsilon \sim \frac{1}{Z(\mu,\sigma)} \exp\left(-\frac{d(y,\mu)^2}{2\sigma^2}\right)$

and $Z(\mu,\sigma) = \int_{\mathcal{M}} \exp\left(-\frac{d(y,\mu)^2}{2\sigma^2}\right)$ is the normalization factor.

Estimation of CDTs and Parallel Transport [2]

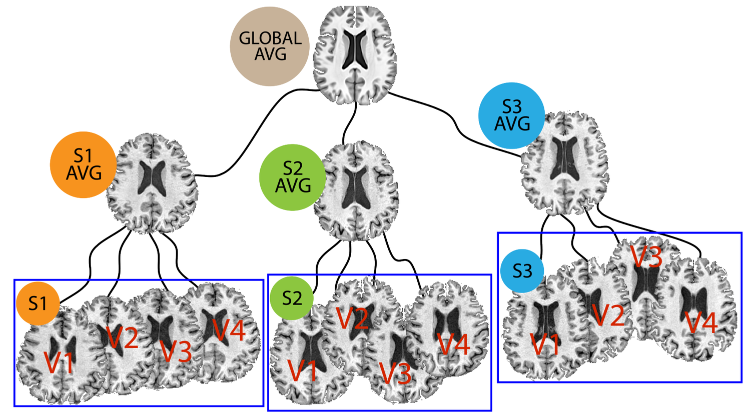

Figure: Schematic for generating least biased global coordinate system for the longitudinally acquired imaging data. Visits V1-V4 are averaged first which are then used to estimate the global average.

Features for Morphometric Changes

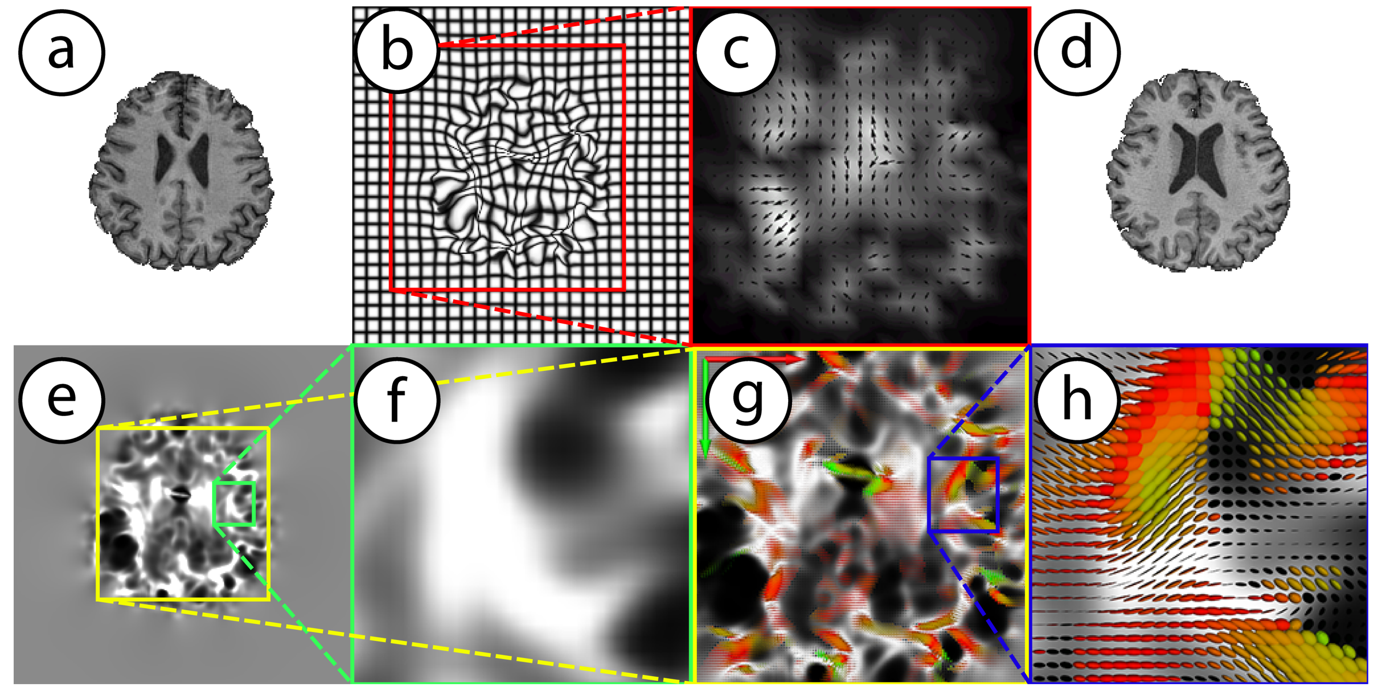

Figure: **An example panel of data generated in morphometric studies.** (a, d) The moving and fixed brain image respectively. (b) Warped spatial grid to move (a) to (d). (c) Vector field of local deformations. (e, f) A map of the *det*(J) of the deformation field. (g, h) The Cauchy deformation tensor field (CDTs) ($\sqrt{J^TJ}$). Among the different features of brain morphology that can be analyzed, CDTs are the focus of this paper.

Algorithm

1: Calculate the Fréchet mean $\bar{y} \in \mathcal{M}$ of population.
2: Calculate the Fréchet mean for each subject $\bar{y}_i \in \mathcal{M}$.
3: Estimate the main longitudinal change direction η
4: Calculate subject-specfic base points (random effects) $B_i = \mathrm{Exp}(B, U_i^*)$, where $U_i^* = \mathrm{argmin}_{U_i} \mathrm{d}(\bar{y}_i, \mathrm{Exp}(B, U_i))^2 + \lambda_{U_i}\Vert U_i\Vert_B^2$.
5: $y^{\wr}_{ij} = \Gamma_{B_i \to I}\mathrm{Log}(B_i, y_{ij})$.
6: **while** until convergence **do**
7: Calculate the common speed of change $V = c\eta$ and common time intercept $t_0 = b/c$ with fixed all other variables by

$$\begin{bmatrix} \sum_{ij} q_i^T q_i & \sum_{ij} p_{ij}^T q_i \\ \sum_{ij} p_{ij}^T q_i & \sum_{ij} p_{ij}^T p_{ij} \end{bmatrix} \begin{bmatrix} b \\ c \end{bmatrix} = \begin{bmatrix} \sum_{ij} q_i^T y^{\wr}_{ij} \\ \sum_{ij} p_{ij}^T y^{\wr}_{ij} \end{bmatrix},$$

where $b := t_0 c$, $q_i := \eta(1 - \alpha_i)$, $p_{ij} := \eta(\alpha_i x_{ij} - \alpha_i \tau_i)$.

8: Given V, t_0, calculate the subject-specific acceleration α_i, and time-shift τ_i by generalized least square estimation with the priors for α_i and $\tau_i = d_i/\alpha_i$

$$\begin{bmatrix} \sum_j W_{ij}^T W_{ij} & -\sum_j W_{ij}^T V \\ \sum_j W_{ij}^T V & -\sum_j V^T V \end{bmatrix} \begin{bmatrix} \alpha_i \\ d_i \end{bmatrix} = \begin{bmatrix} \sum_j \Upsilon_{ij}^T W_{ij} \\ \sum_j \Upsilon_{ij}^T V \end{bmatrix},$$

where $\Upsilon_{ij} := y^{\wr}_{ij} - Vt_0$, $W_{ij} := V(X_{ij} - t_0)$ and $d_i = \alpha_i \tau_i$.
9: **end while**

Cauchy Deformation Tensors vs. det(J)

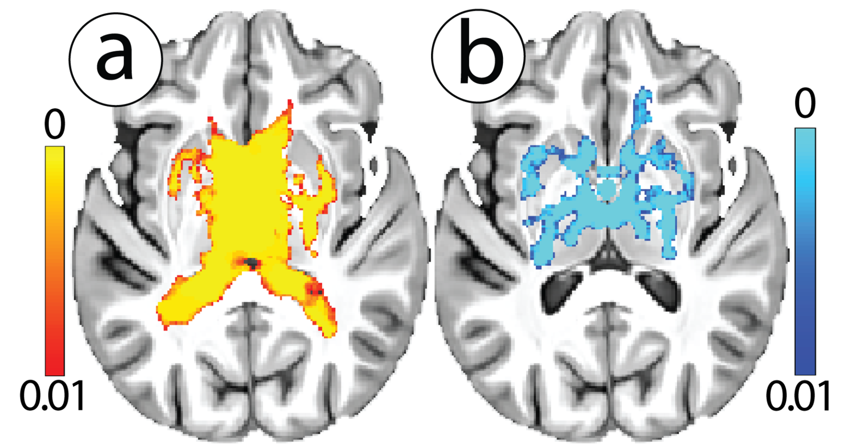

Figure: Results of Cramér's test showing voxels that are different between middle and old age groups ($p < 0.01$) from (a) CDTs and (b) det(J).

Relative Speed Maps of Morphometric Changes

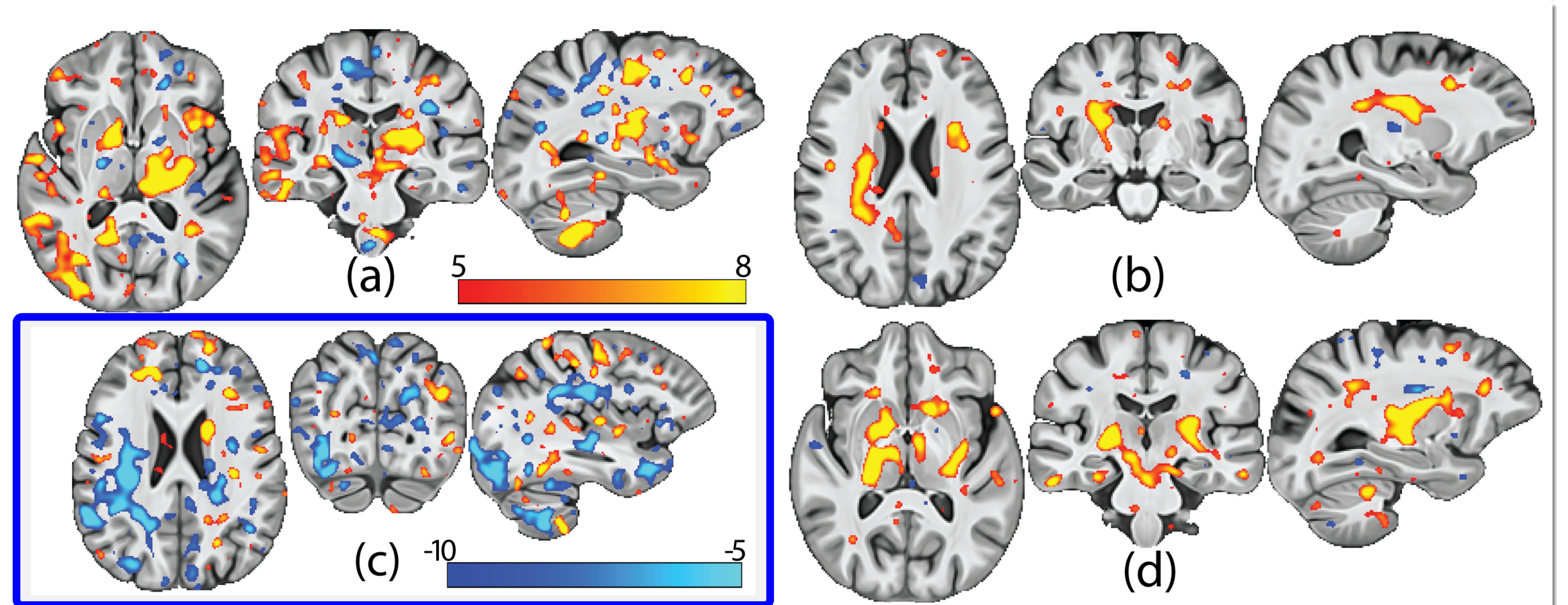

Figure: **Representative acceleration (α_i) maps from RNLMM.** (a) Female, APOE-. (b) Female, APOE+. (c) Male, APOE-. (d) Male, APOE+. The male with no APOE risk shows slower progression (blue regions) compared to the population average.

Group Difference in Subject-Specific Spatial Shifts

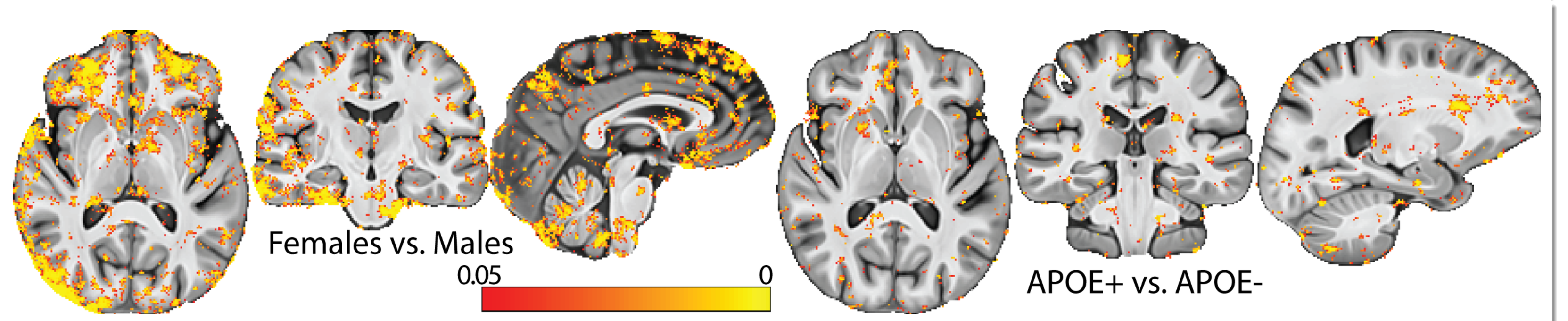

Figure: P-value maps of group differences in random effects (U_i). Left: Gender. Right: APOE group {APOE+, APOE-}. Group differences can be effectively captured by RNLMM based on CDT.

Group (Gender) Difference in U_i Averaged in ROIs

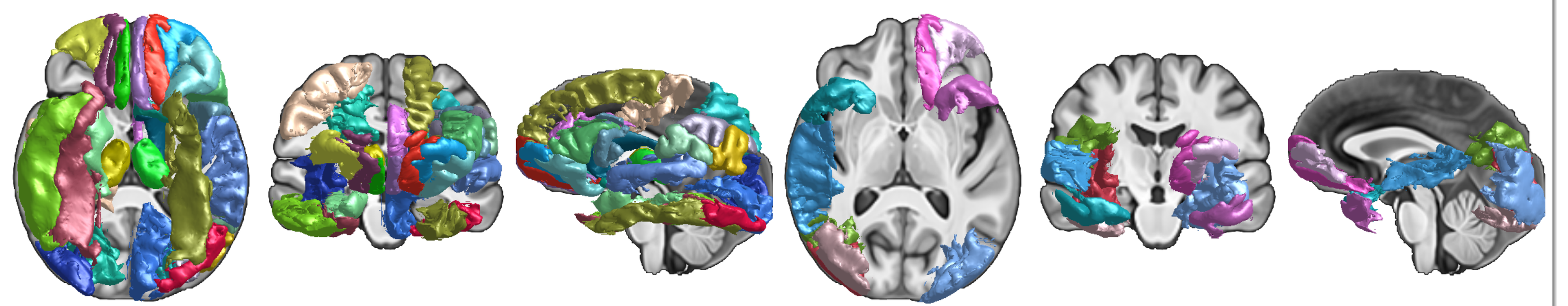

Figure: Gender difference. RNLMM based on CDTs (left) found significant difference from 29 ROIs whereas RNLMM based on determinants (right) found 9 ROIs.

Reference

[1] H.J. Kim et al., "Multivariate General Linear Models (MGLM) on Riemannian Manifolds with Applications to Statistical Analysis of Diffusion Weighted Images." CVPR, 2014.

[2] M. Lorenzi and X. Pennec, "Efficient parallel transport of deformations in time series of images: from Schilds to pole ladder." JMIV, 2014.

[3] Schiratti et al., "Learning spatiotemporal trajectories from manifold-valued longitudinal data." NIPS, 2015.

Research supported by NIH grants AG040396, AG021155, BRAIN Initiative R01-EB022883, UW ADRC AG033514, UW ICTR 1UL1RR025011, Waisman IDDRC U54-HD090256, UW CPCP AI117924, and NSF grants: CAREER award 1252725 (VS), IIS 1525431 (BCV).